THE JOURNAL OF PHYSICAL CHEMISTRY B

Article

pubs.acs.org/JPCB

Coupling of Carbon Dioxide Stretch and Bend Vibrations Reveals Thermal Population Dynamics in an Ionic Liquid

Chiara H. Giammanco, Patrick L. Kramer, Steven A. Yamada, Jun Nishida, Amr Tamimi, and Michael D. Fayer*

Department of Chemistry, Stanford University, Stanford, California 94305, United States

ABSTRACT: The population relaxation of carbon dioxide dissolved in the room temperature ionic liquid 1-ethyl-3-methylimidazolium bis(trifluoromethylsulfonyl)imide ($EmimNTf_2$) was investigated using polarization-selective ultrafast infrared pump−probe spectroscopy and two-dimensional infrared (2D IR) spectroscopy. Due to the coupling of the bend with the asymmetric stretch, excitation of the asymmetric stretch of a molecule with a thermally populated bend leads to an additional peak, a hot band, which is red-shifted from the main asymmetric absorption band by the combination band shift. This hot band peak exchanges population with the main peak through the gain and loss of bend excitation quanta. The isotropic pump−probe signal originating from the unexcited bend state displays a fast, relatively small amplitude, initial growth followed by a longer time scale exponential decay. The signal is analyzed over its full time range using a kinetic model to determine both the vibrational lifetime (the final decay) and rate constant for the loss of the bend energy. This bend relaxation manifests as the fast initial growth of the stretch/no bend signal because the hot band (stretch with bend) is "over pumped" relative to the ground state equilibrium. The nonequilibrium pumping occurs because the hot band has a larger transition dipole moment than the stretch/no bend peak. The system is then prepared, utilizing an acousto-optic mid-infrared pulse shaper to cut a hole in the excitation pulse spectrum, such that the hot band is not pumped. The isotropic pump−probe signal from the stretch/no bend state is altered because the initial excited state population ratio has changed. Instead of a growth due to relaxation of bend quanta, a fast initial decay is observed because of thermal excitation of the bend. Fitting this curve gives the rate constant for thermal excitation of the bend and the lifetime, which agree with those determined in the pump−probe experiments without frequency-selective pumping.

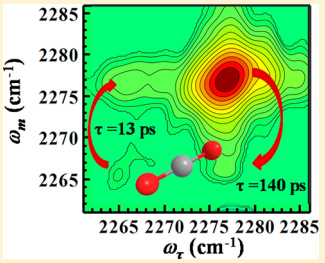

I. INTRODUCTION

Room temperature ionic liquids (RTILs) are novel compounds: salts that remain molten at room temperature. They have been proposed or used for various applications including electrochemistry, separations, and catalysis.[1] Another potential use is in carbon capture applications.[2,3] Since both the cation and anion chemical structure can be tuned, there exist a vast number of RTILs that have distinct properties.[4] Utilizing RTILs to their fullest potential requires an understanding of the RTIL structures that give rise to desired properties so that these can be enhanced and deleterious properties can be minimized.

Here we investigate the population relaxation of carbon dioxide in the ionic liquid 1-ethyl-3-methylimidazolium bis(trifluoromethylsulfonyl)imide ($EmimNTf_2$, Figure 1). $EmimNTf_2$ is a well studied RTIL that has been proposed for carbon capture. While much research has focused on the solubility and diffusion time of CO_2 through thin films of the ionic liquid,[5−9] very little research has focused on the exact dynamics of the molecule in solution. Understanding these short time scale interactions and dynamics can be critical in designing task-specific ionic liquids. To access these extremely fast motions, ultrafast vibrational spectroscopy was used. Both two-dimensional infrared spectroscopy (2D IR) and polarized pump−probe experiments were conducted. This paper focuses on understanding the vibrational population relaxation of carbon dioxide solvated in an IL matrix. The full dynamic picture, including CO_2 reorientation and the structural fluctuations in the local environment, will appear in subsequent publications.

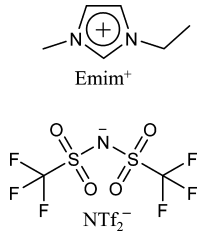

Figure 1. Structure of the ionic liquid used: 1-ethyl-3-methylimidazolium bis(trifluoromethylsulfonyl)imide, abbreviated as $EmimNTf_2$ throughout the paper.

Vibrational relaxation has been studied extensively. Typically the vibration in question couples both to the other modes of the molecule as well as bath modes of the solvent.[10] Relaxation into these modes occurs much faster than radiative decay, such that the radiative decay can be neglected. Several studies[11,12] of pure water have investigated how vibrational energy is dissipated in the system, typically by selectively pumping and

Received: November 23, 2015
Revised: December 22, 2015
Published: January 5, 2016

DOI: 10.1021/acs.jpcb.5b11454
J. Phys. Chem. B 2016, 120, 549−556

probing both the water molecule's stretch and bend modes and watching the energy exchange. It has been found that the stretching vibration primarily relaxes into the bend overtone, whose energy is then dissipated into the quasi-continuous bath modes.[12−14] For carbon dioxide in ionic liquid media, the bend frequency is much further detuned from the stretching mode, and it is not as strongly coupled to the solvent since the IL does not extensively hydrogen bond like water does. The bend of carbon dioxide[15] is much lower in frequency (660 cm^{-1}) than that of water[16] (1650 cm^{-1}), and it lies in a region of the spectrum in which the RTIL absorption background is substantial. The large solvent background absorption and the low frequency make it difficult to directly measure the bend dynamics.

In the CO_2/RTIL system we can take advantage of the stretch/bend mode coupling to access the bend relaxation dynamics and understand the observed stretch population dynamics. The bending mode of $^{12}CO_2$ (660 cm^{-1}) has relatively low frequency such that at room temperature ($k_BT \approx$ 200 cm^{-1}) the bend is thermally excited for a minor but non-negligible fraction of carbon dioxide molecules. Owing to the anharmonic coupling of the bend mode and the antisymmetric stretch, the resonant frequency of the stretching mode for CO_2 molecules with a thermally excited bend is red-shifted from those with the bend in the ground state. The stretch absorption arising from the thermally excited bend is referred to as "hot band" in later sections. Indeed, when infrared absorption spectrum of the antisymmetric stretching mode is observed carefully, there is small but distinguished side peak which is shifted by ∼11 cm^{-1} from the main peak (see Figure 2), which

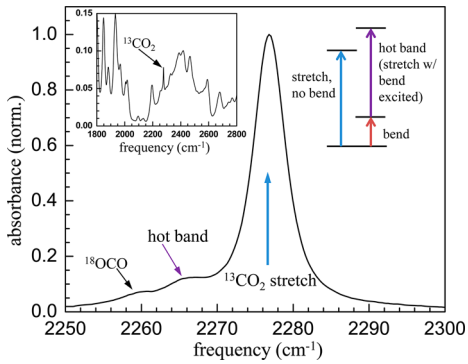

Figure 2. FT-IR normalized difference spectrum of the asymmetric stretching mode of $^{13}CO_2$ in $EmimNTf_2$. The shoulder to the red side is primarily due to the hot band absorption of the asymmetric stretch when the bend is thermally excited. It is shifted to lower frequency from the main asymmetric stretch absorption by the combination band shift. The energy level diagram shows the excitation of the stretch from the ground state (blue arrow), the excitation of the bend from the ground state (red arrow), and the excitation of the stretch when the bend has already been excited—the hot band (purple arrow). The inset shows the spectrum over a broader region around the $^{13}CO_2$ stretch absorption without background subtraction or normalization.

is the hot band mentioned above. This 11 cm^{-1} is what is known as the combination band shift. The amplitude of the hot band is determined by the number of CO_2 molecules in the bend excited state and also the strength of the transition, which is determined by the magnitude of the transition dipole moment. This stretch transition dipole can differ from that of carbon dioxide with the bend in the ground state. After excitation of both transitions with a short mid-infrared laser pulse, the hot band can then exchange population with the main peak (the stretch/no bend) by the gain and loss of the bend vibrational excitation energy. Monitoring the population dynamics of the stretch/no bend with a time-delayed probe pulse yields information on both vibrational lifetime relaxation of the stretch and population exchange with the other band, that is, the bend relaxation time constant and the bend thermal excitation time constant. The time constant for thermal excitation of a vibration is not generally a direct experimental observable.

II. EXPERIMENTAL PROCEDURES

The room temperature ionic liquid $EmimNTf_2$ was purchased from IoLiTec Ionic Liquids Technologies Inc., dried for a week by heating to 60 °C under vacuum, and stored in a nitrogen glovebox. Isotopically labeled $^{13}CO_2$ (99% purity) was purchased from Icon Isotopes and used without further purification. Samples consisted of a drop of solution sandwiched between two 3 mm thick CaF_2 windows separated by a Teflon spacer. The sample cell was assembled in a dry atmosphere to prevent water uptake by the ionic liquid. Infrared spectra were taken with a Thermo Scientific Nicolet 6700 FT-IR spectrometer. Background spectra were taken of samples under identical conditions, but without $^{13}CO_2$ added. The background spectrum was subtracted from the $^{13}CO_2$-containing sample spectra. The carbon dioxide concentration was kept sufficiently low such that vibrational excitation transfer between CO_2 molecules was unlikely to occur.

2D IR spectra and IR pump−probe measurements were recorded using two experimental 2D IR setups, for which the layout and data acquisition procedures have been described in detail previously.[17,18] Briefly, a Ti:sapphire oscillator/regenerative amplifier system was run at a 1 kHz repetition rate and pumped a BBO optical parametric amplifier (OPA). The signal and idler output of the OPA were difference-frequency mixed in a $AgGaS_2$ crystal to create mid-IR pulses.

The mid-IR beams propagated in an enclosure that was purged with air scrubbed of water and carbon dioxide to minimize absorption of the IR. Despite this, some atmospheric $^{12}CO_2$ absorption remained. Therefore, $^{13}CO_2$ was used in the experiments. The isotopic labeling shifted the probe absorption away from the $^{12}CO_2$ absorption, so that it did not distort the $^{13}CO_2$ data in the spectral range of interest.

The IR light was collimated and then split into two beams for both the pump−probe and vibrational echo measurements. To collect pump−probe data, the pump beam polarization was rotated 45° relative to that of the probe (horizontal polarization) using a half-wave plate and followed by a polarizer, and the pump pulse was chopped at half the laser repetition rate. The two beams crossed in the sample, and the probe polarization was resolved either parallel or perpendicular to the pump beam by a computer controlled polarizer before detection. The vibrational echo experiments were conducted in the pump−probe geometry with a Germanium acousto-optic mid-infrared pulse shaper. Three incident pulses, the first two of which (the pump) are generated collinearly by the pulse shaper, stimulated the emission of the vibrational echo in the phase-matched direction, which is collinear with the third (probe) pulse. The probe serves as the local oscillator for heterodyne detection of the echo signal. The signal (probe or echo) was dispersed by a spectrograph (300 line/mm grating)

DOI: 10.1021/acs.jpcb.5b11454
J. Phys. Chem. B 2016, 120, 549−556

and detected on a 32 pixel, liquid nitrogen cooled, mercury−cadmium−telluride array.

The two ultrafast infrared spectroscopy setups used in this investigation differed in the mid-IR bandwidth generated (and thus minimum possible pulse length), pulse shaping functionality, and the pixel width of the array detector. The first system[17] used was employed for pump−probe measurements. It afforded greater time resolution as it had shorter pulses (~70 fs). The second system[18] employed a pulse shaper in the pump−probe geometry. Though it did not have as high a time resolution, it did generate significantly more IR power at the $^{13}CO_2$ probe wavelengths and was outfitted with an array detector with thinner pixels (0.1 mm vs 0.5 mm). The narrow pixels permitted the data to be acquired with greater spectral resolution. The pulse shaper allowed phase cycling and collection of echo interferograms in the partially rotating frame for scatter removal and rapid data acquisition. The pulse shaper can also modify the spectrum of the pump pulse such that one vibrational mode is selectively pumped.[19] As demonstrated in the later section, in some of the measurements we created a hole in the pump spectrum such that we selectively pumped the main 2277 cm^{-1} antisymmetric mode without pumping the side hot band (Figure 6).

III. RESULTS AND DISCUSSION

A. Absorption Spectra. Carbon dioxide is a linear molecule with four vibrational modes: a symmetric stretch, an asymmetric stretch, and a doubly degenerate bend. The symmetric stretch displacement does not change the dipole moment, and therefore the mode is not IR active. In this study, the asymmetric stretch is monitored. The peak of unlabeled carbon dioxide ($^{12}CO_2$) shifts from 2350 cm^{-1} in the gas phase to 2342 cm^{-1} when dissolved in the ionic liquid.[15] As can be seen in the absorption spectrum (Figure 2), the isotopically labeled $^{13}CO_2$ absorbs at 2277 cm^{-1}. We chose to use the isotopically labeled carbon dioxide to eliminate the effects of atmospheric CO_2.

The main absorption band of $^{13}CO_2$ in EmimNTf$_2$ is fairly narrow (see Figure 2), with a 5 cm^{-1} full width at half-maximum (fwhm). This is somewhat narrower than the 7 cm^{-1} fwhm absorption spectrum of CO_2 in water,[20] but the narrowing of the probe absorption peak in an ionic liquid versus another solvent is not unusual.[21,22] The narrow band suggests that either the vibrational frequency does not change substantially as the carbon dioxide experiences different environments in the ionic liquid (perhaps because the coupling is weak) or the molecule is found in only a narrow range of structural configurations. To the red side of the line there is a noticeable shoulder (see Figure 2). It is present both for isotopically labeled and unlabeled CO_2.[23] Often this might be interpreted as a second population in solution, possibly due to a second environment. However, it has been shown[23] that this shoulder is a hot band, a result of the thermally populated bend that is coupled to the asymmetric stretch. Thus, the absorption shows up red-shifted from the main peak by the combination band shift. An additional very small peak is seen further to the red. We attribute this to molecules that contain an ^{18}O instead of two ^{16}Os, as the $^{13}CO_2$ gas contains 1% ^{18}O, according to the supplier's specifications. This peak is shifted far enough from the main peak and has a very low amplitude such that it does not interfere with the experiments.

B. Population Relaxation. The polarization-selective pump−probe experiment permits the determination of both the population relaxation (vibrational lifetime) and the anisotropy (reorientation dynamics). The polarized probe signals parallel, $S_{\parallel}(t)$, and perpendicular, $S_{\perp}(t)$, to the pump are measured. These signals can be expressed in terms of population relaxation, $P(t)$, and the second Legendre polynomial orientational correlation function of the vibrational transition dipole, $C_2(t)$:

$$S_{\parallel} = P(t)[1 + 0.8C_2(t)] \quad (1)$$

$$S_{\perp} = P(t)[1 - 0.4C_2(t)] \quad (2)$$

The population relaxation, free of orientational relaxation, is given by

$$P(t) = (S_{\parallel}(t) + 2S_{\perp}(t))/3 \quad (3)$$

At early times, a nonresonant signal, which tracks the pulse duration, overwhelms the desired signal from the resonant vibrations. Thus, only the data after 300 fs is used. Other than in signal intensity, the population relaxation does not vary across the band. No evidence of multiple populations was found, either from FT-IR peaks or populations with discernibly different lifetimes resulting in multiple exponential lifetime decays. Thus, analyzing one detection wavelength is sufficient to describe the dynamics.

In Figure 3, the population relaxation at the center of the peak is plotted (black curve) along with a single exponential fit

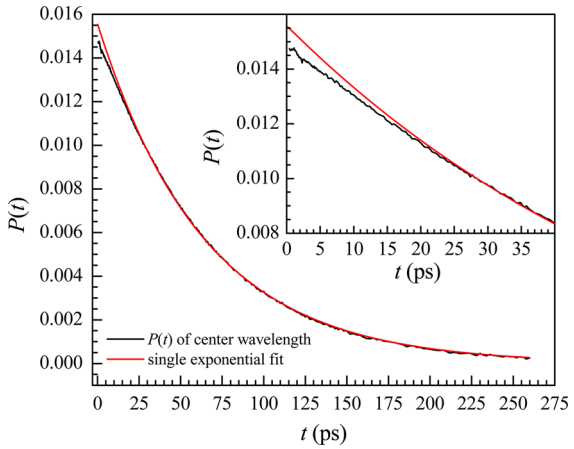

Figure 3. Plot of the $^{13}CO_2$ stretch population relaxation data (black curve) at the center of the band (2277 cm^{-1}). A single exponential fit (red curve) to the data from 50 ps to the end is plotted and extrapolated back to time zero, yielding a vibrational lifetime of 64 ± 2 ps. A deviation from the fit can be seen at short time. The inset shows an enlargement of the early time data (black curve) and the lifetime single exponential fit (red curve). The deviation from the single exponential decay is clear.

(red curve). Notice that at early time the data exhibit behavior other than that of a single exponential decay (see inset). By fitting a single exponential from 50 ps to the end of the recorded decay, $^{13}CO_2$ was found to have a vibrational lifetime of 64 ± 2 ps. From this fit extrapolated back in time to $t = 0$, it is clear that a growth is occurring at early time. The mechanism for the growth at relatively short times needs to be determined from among several possibilities. The non-Condon effect, in which different frequencies in a single band can have different transition dipole moments, can lead to unequal pumping across the band. If molecules that absorb on the red side of the line

DOI: 10.1021/acs.jpcb.5b11454
J. Phys. Chem. B 2016, 120, 549−556

have larger transition dipoles (as is typically the case for hydrogen-bonded hydroxyls),[22,24] overpumping on the red side would result in a growth at bluer wavelengths and a corresponding decay on the red side. This red decay and blue growth is a result of spectral diffusion, which brings into equilibrium the initial nonequilibrium distribution of population across the line.[22,25] However, we observe a uniform growth across the band, which rules out a non-Condon effect and spectral diffusion involvement. Also possible would be contributions from the solvent background. However, the experiment was performed for the neat ionic liquid without any carbon dioxide added, and there was no signal. This leaves the possibility of population transfer, which should be evident in 2D IR spectra, and is investigated below.

C. 2D IR Experiments. Figure 4 shows two-dimensional infrared (2D IR) spectra[26] at a short time, T_w = 0.5 ps, and a longer time, T_w = 5 ps. The dashed line in each panel is the diagonal. While a great deal of dynamical information can be obtained from 2D IR spectroscopy, here we are only interested in the growth of off-diagonal peaks as the waiting time (T_w) is increased. In the top panel, at short time the large band on the diagonal (upper right) is from the stretch with no bend excited. The much smaller peak (lower left) is from the stretch with the bend excited. As in the absorption spectrum (Figure 2), this small peak is at lower frequency because of the combination band shift of the stretch when the bend is excited.

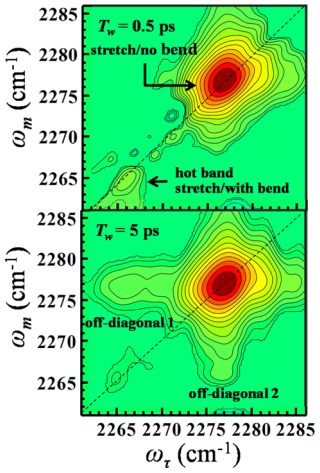

Figure 4. Two-dimensional infrared (2D IR) spectra of $^{13}CO_2$ in $EmimNTf_2$ at two waiting times, T_w = 0.5 and 5 ps. The dashed lines are the diagonals. Off-diagonal peaks grow in by the longer waiting time. The growth of the off-diagonal confirms the transfer of population from the hot band to the main band and vice versa. Contour lines are on a logarithmic scale to better visualize the small peaks.

In the lower panel of Figure 4, two new off-diagonal peaks have grown in. Off-diagonal 1 arises from relaxation of the bend to the ground state for the stretches that initially had the bend excited. The population moves from the combination band shifted frequency to the frequency of the stretch with no bend excited along the ω_m (vertical) axis. Off-diagonal 2 arises from bends becoming thermally excited for stretches that initially did not have the bend excited. The population moves along the ω_m (vertical) axis from the stretch frequency to the combination band shifted stretch frequency, which occurs when the bend is excited. These off-diagonal peaks are the result of population transfer during the waiting time from one population to the other and thus are the result of either losing or gaining excitation quanta of the bend. These spectra are consistent with the ones presented by Brinzer et al. for $^{12}CO_2$ in 1-butyl-3-methylimidazolium (Bmim) based ionic liquids.[23] They also observed the cross peaks to grow in with time and attributed it to dynamic exchange. Though Bmim has a longer alkyl tail than Emim and a different isotope of carbon dioxide was used, the systems are very similar.

Detailed analysis of the full time dependence of the shape of the 2D IR spectra will be presented in a forthcoming paper. The goal of introducing them here is to demonstrate that off-diagonal peaks between the fundamental asymmetric stretch and hot band grow in with time. In principle, these spectra can be analyzed using the same techniques developed by Fayer et al.[27] for quantifying chemical exchange via changes in peak volume of the 2D IR spectra. However, the weak hot band signal that is near the noise level and the small amount of transfer, compared to the size of the main peak, make this analysis prone to error. The frequency-resolved pump−probe experiment is equivalent to measuring the projection of the 2D-IR onto the ω_m axis.[28,29] Therefore, when the population dynamics data are fit, the growth of these off-diagonal peaks are a contribution to the data in addition to simple population relaxation of the excited stretch to the ground state. Frequently such off-diagonal peaks do not contribute to the vibrational relaxation signal because the relative populations of vibrationally excited states are determined by the ground-state thermal equilibrium populations. When this is the case, the same amount of population moves from stretch/with bend to stretch/no bend as moves from stretch/no bend to stretch/with bend. For the main band in a 2D spectrum, which is monitored in the pump−probe experiments, as many molecules transfer into the off-diagonal peak as transfer out of the diagonal peak per unit time, and no net dynamical signal from this exchange is observed. To see this exchange process, the system must initially be prepared not in thermal equilibrium. If the system is prepared out of equilibrium, the rates will be unequal, and the rate constants of the transfer processes will impact the pump−probe population relaxation measurements.

D. Rate Equation Model. What causes the initial nonequilibrium situation? If the transition dipoles of the two peaks, stretch and hot band (see Figure 2), are not equal, then one population will be pumped more than the other. The result is an initial nonthermal equilibrium distribution of excited states in the two bands following the pump pulse. As discussed quantitatively below, the hot band transition dipole is larger than that of the stretch with no bend excited. When pumped, this gives rise to an initial nonthermal equilibrium number of excitations in the two bands, with an excess of population in the hot band (stretch with bend excited).

The observed dynamics can be modeled with a system of coupled rate equations. The process of the loss and gain of the bend can be written as

$$N_{1,0} \underset{k_g}{\overset{k_b}{\rightleftharpoons}} N_{0,0} \tag{4}$$

where $N_{0,0}$ is the number of molecules in the vibrational ground state, $N_{1,0}$ is the number of molecules with only one bending mode excited (the first number refers to quanta of the bend, the second to quanta of the stretch), k_b is the bend lifetime decay rate constant, and k_g is the rate constant for the thermal excitation of one bending mode. At equilibrium $k_g N_{0,0}(t)$ =

DOI: 10.1021/acs.jpcb.5b11454
J. Phys. Chem. B 2016, 120, 549−556

$k_b N_{1,0}(t)$. This is the system that exists in thermal equilibrium before the sample has been excited by the IR pump pulse. The number fraction of particles at energy ε (641 cm^{-1} for the $^{13}CO_2$ bend) is given by the Bose–Einstein distribution,

$$n(\varepsilon) = \frac{g_\varepsilon}{\exp[\varepsilon/k_B T] - 1}$$

where g_ε is the level degeneracy (2 for the bend), k_B is Boltzmann's constant, and T is temperature. Thus, the population ratio of the ground and thermally excited bend levels can be written

$$\frac{N_{1,0}}{N_{0,0}} = \frac{n(\varepsilon)}{1 - n(\varepsilon)} = \frac{k_g}{k_b} \equiv a \tag{5}$$

assuming that the multiple excitations of the bend are so sparsely populated at room temperature that they can be neglected. That is, all the molecules can be found in the either the ground state or one bend excited state. We define this ratio to be a.

When the asymmetric stretch is excited, we can write the following system of equations to describe the dynamics, where the vibrational lifetime decay rate constant, k_l, of the asymmetric stretch has been added as a decay path.

$$\begin{cases} \dfrac{dN_{0,1}(t)}{dt} = -k_g N_{0,1}(t) + k_b N_{1,1}(t) - k_l N_{0,1}(t) \\ \dfrac{dN_{1,1}(t)}{dt} = k_g N_{0,1}(t) - k_b N_{1,1}(t) - k_l N_{1,1}(t) \end{cases} \tag{6}$$

$N_{0,1}$ is the number of molecules with only the stretch excited and $N_{1,1}$ is the number of molecules with both bend and stretch excited. Both peaks (the fundamental and hot band) are taken to decay with the same rate constant, k_l. While this is an approximation, the small shift between the peaks (11 cm^{-1}) indicates that both populations see essentially the same density of states of the bath, resulting in the same lifetime.[10]

As mentioned above, to observe a growth in the pump–probe signal at relatively short times (see Figure 3), excitation of the main stretch band and the hot band must result in a nonequilibrium population ratio. To observe a growth, the hot band transition dipole must be larger than that of the main band. The larger transition dipole will give rise to an excess population in the hot band peak and a subsequent net flow of population from the hot band to the main band until thermal equilibrium is established.

To determine the difference in the transition dipoles, we examined the FT-IR spectrum (Figure 2). For linear spectra, the absorbance follows Beer's law, $A = \alpha l C$, where α is the molar absorptivity and is proportional to the transition dipole of the vibration (μ) squared, l is the path length, and C is the concentration. Since both populations exist in the same sample, the path lengths are equal. However, the concentration C is not equal; for the main peak, it is proportional to the number of molecules in the ground state, $N_{0,0}$, while for the hot band, it is proportional to the number of molecules in the bend excited state, $N_{1,0}$. We also cannot assume the transition dipoles are the same. Overall, the ratio of stretch absorbance of the two populations is,

$$\frac{A_{0,1}}{A_{1,1}} = \frac{\mu_{nb}^2 N_{1,0}}{\mu_{wb}^2 N_{0,0}} = \frac{\mu_{nb}^2}{\mu_{wb}^2}\frac{1}{a} \tag{7}$$

where μ_{nb} is the transition dipole for the stretch with no bend excited (the main peak), and μ_{wb} is the transition dipole for the stretch with bend excitation (the hot band peak).

The absorbance areas were obtained from multipeak fits to the linear spectrum shown in Figure 2, and the population ratio, a, was computed from eq 5 above. The ratio of the square of the transition dipoles, m, is then found to be

$$m \equiv \left(\frac{\mu_{nb}}{\mu_{wb}}\right)^2 = \frac{A_{0,1}}{A_{1,1}} a = (8.2 \pm 0.6)a \tag{8}$$

For $^{12}CO_2$ in BmimNTf2, the bend frequency is 660 cm^{-1}.[15] In air, the bend is 667 cm^{-1}, and the $^{13}CO_2$ bend is shifted to lower frequency by 19 cm^{-1}.[30] It is reasonable to assume that the shift will be virtually the same in the IL, resulting in the $^{13}CO_2$ in EmimNTf2 having a frequency of 641 cm^{-1}. The calculations presented below are essentially unchanged for a ±5 cm^{-1} change in the bend frequency. Using 641 cm^{-1}, a can be computed, and $m = 0.84 \pm 0.06$, which clearly demonstrates that the hot band transition dipole (stretch with thermally excited bend) is larger than the transition dipole of the main peak (stretch without an excited bend). Thus, the hot band is over pumped and there is an initial excess population of the hot band, which will relax toward equilibrium giving rise to the observed growth in the main peak's pump–probe signal (Figure 3). This value of m provides the necessary quantitative ratio of the square of the transition dipoles used in the following calculations.

To model the data, we solve the system of differential eqs (eq 6) with the appropriate initial condition. At time $t = 0$, the number of molecules in a particular population is proportional to the absorbance, $N \propto A$. Thus, taking the ratio of the two populations we can write

$$\frac{N_{0,1}(0)}{N_{1,1}(0)} = \frac{A_{0,1}}{A_{1,1}} = \frac{m}{a} \Rightarrow N_{0,1}(0) = \frac{m}{a} N_{1,1}(0) \tag{9}$$

The pump–probe decay from the $N_{1,1}$ population (hot band) suffers from low signal-to-noise because of its small amplitude, overlap with the $N_{0,1}$ population signal, and additional overlap from the 1 to 2 transition of the $N_{0,1}$ population. Thus, only the signal from the $N_{0,1}$ population is fit. Solving, using the initial condition given in eq 9, and normalizing to the initial signal, gives

$$\frac{N_{0,1}(t)}{N_{0,1}(0)} = \frac{\exp(-k_l t)}{m(k_g + k_b)}\{k_b(m + a) + (mk_g - ak_b)\exp[-(k_g + k_b)t]\} \tag{10}$$

As was determined in eq 5, $k_g = ak_b$. Making this replacement and switching to time constants, which are related to the rate constant by $\tau_i = 1/k_i$, yields a simplified expression:

$$\frac{N_{0,1}(t)}{N_{0,1}(0)} = \frac{\exp(-t/\tau_l)}{m(a + 1)}\{m + a[1 + (m - 1) \times \exp(-(a + 1)t/\tau_b)]\} \tag{11}$$

This equation can then be fit to the data where m and a are both known and so the only free parameters are a normalization amplitude, the lifetime, and the time constant for the bend decay. In fact, the lifetime is also known from fitting the data at long time. The fit to the full data range with

DOI: 10.1021/acs.jpcb.5b11454
J. Phys. Chem. B 2016, 120, 549–556

the model yields the same lifetime as the long-time, single exponential lifetime fit.

The data and fit are shown in Figure 5. The bend lifetime is found to be $\tau_b = 13 \pm 2$ ps. The fit describes the data very well,

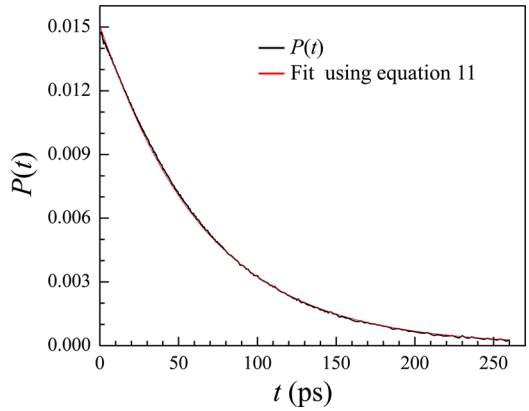

Figure 5. Population relaxation, $P(t)$, data (black curve) measured at the asymmetric stretch absorption peak frequency (2277 cm^{-1}), along with the corresponding fit (red curve) to the kinetic model (eq 11). The fit has only two adjustable parameters, τ_b, the bend lifetime and an overall normalization constant. The stretch lifetime was obtained from the single exponential fit at long times (see Figure 3).

even though there is some error in the transition dipole ratio and the assumption that the antisymmetric stretch lifetimes, τ_1, of the two populations are equal.

The experiments and analysis explain the nonexponential early time pump−probe data and yield the lifetimes of the asymmetric stretch and the bend. Another experiment can be performed that measures the time constant for thermal excitation of the bend and tests the model. In general, it is not possible to measure the time constant for thermal excitation by measuring the bend directly because there is no way to define $t = 0$. Here we use an approach that takes advantage of the ability of the pulse shaping 2D IR spectrometer to control the excitation pulse spectrum in the pump−probe experiment.

We performed the pump−probe experiment such that the hot band was not pumped, but the asymmetric stretch main peak (no bend excitation) was excited, and its population dynamics were observed. Using the pulse shaping system, a hole was cut out of the incident pump spectrum; the resulting spectrum is displayed in Figure 6. Figure 6 shows the full IR pulse spectrum (black curve), the spectrum with the hole (red curve), and the $^{13}CO_2$ stretch absorption spectrum (blue curve). The hole in the IR pump spectrum essentially eliminates pumping the hot band but still pumps the main peak. Pumping with the hole in the spectrum changes the initial conditions. Instead of over pumping the hot band because of its larger transition dipole, we now do not pump the hot band.

The inset in Figure 7 shows the shorter time portion of the data (black curve) and a single exponential fit to the long time portion (50 to 300 ps) of the data (red curve). The red curve has the same vibrational lifetime decay, $\tau_1 = 64 \pm 2$ ps, as found previously. The data at short time is above the lifetime curve but decays quickly to meet the previously determined lifetime decay. Pumping only the main peak results in two decay pathways at shorter times. In addition to the lifetime decay, the population will decay as the bend becomes excited. The stretch with no bend is the only transition excited initially. For this

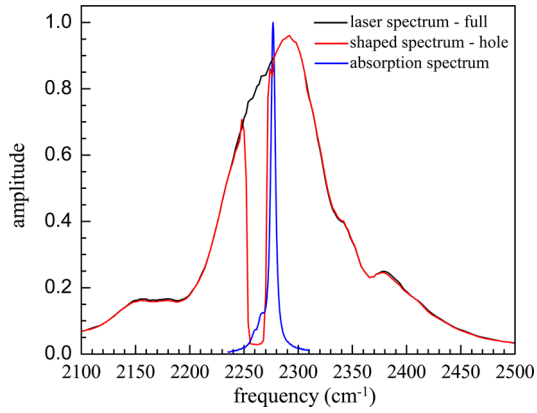

Figure 6. Spectrum of the full pump laser pulse (black curve) and the spectrum of the pulse with a hole in the frequency distribution (red curve) that eliminates pumping of the hot band. The absorption spectrum of the $^{13}CO_2$ asymmetric stretch (blue curve) is superimposed for comparison.

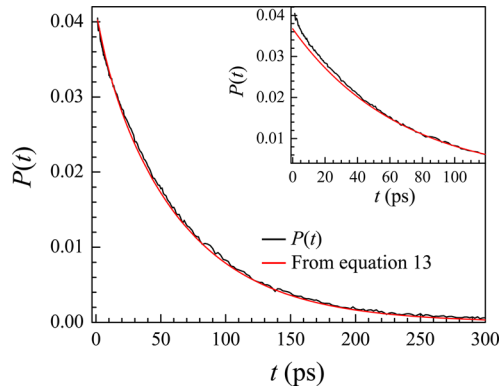

Figure 7. Main portion of the figure shows the full time range of the data (black curve) and the calculation with the time constants fixed (red curve). The inset shows population relaxation, $P(t)$, data (black curve) for the main band taken with the hole in the pump spectrum (Figure 6) to avoid pumping the hot band and the red curve is the lifetime single exponential. The data are above the single exponential curve at short time in contrast to the data in the inset of Figure 3.

ensemble of excited molecules, when a bend becomes thermally excited, population moves from the main peak to the hot band peak. Then the very short time decay rate constant is the sum of the lifetime rate constant and the rate constant for bends to become excited. The result is a decay that is faster than the vibrational lifetime. At later time, as the hot band is populated by thermal excitation of the bend, the bends will decay and return population to the main peak. The system will come to equilibrium and the additional pathway influencing the observed population decay will cease to contribute.

By pumping only the main band using the pump pulse with the spectral hole to eliminate pumping the hot band, the initial condition is $N_{1,1}(0) = 0$, as there is no population in the hot band. Solving the differential equations again and normalizing gives

$$\frac{N_{0,1}(t)}{N_{0,1}(0)} = \frac{\exp(-k_l t)}{(k_g + k_b)}\{k_b + k_g \exp[-(k_g + k_b)t]\} \quad (12)$$

Again, replacing $k_g = ak_b$ from eq 5, which is the detailed balance condition, and switching to time constants gives

DOI: 10.1021/acs.jpcb.5b11454
J. Phys. Chem. B 2016, 120, 549−556

$$\frac{N_{0,1}(t)}{N_{0,1}(0)} = \frac{\exp(-t/\tau_l)}{1+a}\{1 + a\exp[-(1+a)t/\tau_b]\} \quad (13)$$

Note that, because the hot band and the main band overlap to a small extent, the data do not exactly correspond to this ideal case $N_{1,1}(0) = 0$; a small portion of the hot band will be pumped, which will introduce some error. The main portion of Figure 7 shows the data (black curve) and the calculated curve using eq 13 (red curve). There are no adjustable parameters in the calculation other than the overall normalization constant. The time constants were fixed to those found from the fit in Figure 5. The agreement between the calculation and the data is very good. Including the 2-fold degeneracy factor for the bend, the time constant for bend thermal excitation is 140 ps. Thus, the experiments yield the bend lifetime and the time constant for bend thermal excitation without performing a direct experiment on the bend.

IV. CONCLUDING REMARKS

Measurements and analysis of the decay of the IR pump−probe isotropic population signal of the asymmetric stretching mode of $^{13}CO_2$ in the ionic liquid EmimNTf$_2$ have been presented. A single population of CO_2 exists in the solution with the asymmetric stretch spectrum spanning a rather narrow range of frequencies. In addition to the main absorption band, there is a small peak to the red that is a hot band absorption resulting from the combination band shift of the stretch absorption when the bend is also thermally populated. The asymmetric stretch has a lifetime decay of 64 ± 2 ps. However, at relatively short times, the decay is not a single exponential (see Figures 3 and 7). There is a growth at early times that results from transfer of population from the hot band to the main peak caused by thermally excited bends' relaxation to their ground state. This growth is a result of the hot band transition dipole being larger than that of the stretch without bend excitation. The larger hot band absorption causes this population to be over pumped by the IR excitation pulse. The over pumping produces a nonthermal equilibrium distribution of initial populations, which then relaxes to thermal equilibrium by the transfer of the excess hot band (stretch with bend excited) population to the main band (the stretch without bend excitation). This picture is confirmed by 2D IR spectra, which display the growth of off-diagonal peaks that reflect the transfer of population from the hot band to the main band and from the main band to the hot band. The kinetics are modeled with a set of coupled differential rate equations. Fitting the data yields the bend relaxation lifetime, $\tau_b = 13 \pm 2$ ps.

Further evidence for the validity of the model comes from performing the pump−probe experiments with a frequency hole in the pump pulse spectrum such that the hot band is not excited. Instead of showing a growth at early times, these data show an extra decay caused by thermal excitation of the bend, which takes population out of the main peak (stretch with no bend) into the hot band. This experiment permits the direct observation of the time dependence of thermal excitation of the bend. A curve that reproduces these data can be calculated with no adjustable parameters using the same model with the only difference being the initial conditions.

Taken together, these two pump−probe experiments give the asymmetric stretch lifetime, the bend lifetime, and the time constant for thermal excitation of the bend. The experiments provide information on the bend population kinetics without performing an experiment on the bend, which is located at low frequency in a very congested region of the RTIL IR spectrum.

AUTHOR INFORMATION

Corresponding Author

*E-mail: fayer@stanford.edu.

Notes

The authors declare no competing financial interest.

ACKNOWLEDGMENTS

This work was funded by the Division of Chemical Sciences, Geosciences, and Biosciences, Office of Basic Energy Sciences of the U.S. Department of Energy through Grant No. DE-FG03-84ER13251 (C.H.G., P.L.K., M.D.F. and the shorter pulse ultrafast IR spectrometer.) This material is also based upon work supported by the Air Force Office of Scientific Research (AFOSR) under AFOSR Grant No. FA9550-12-1-0050 (S.A.Y., J.N., A.T., M.D.F. and pulse shaping ultrafast IR spectrometer). P.L.K., J.N., and A.T. acknowledge support from Stanford Graduate Fellowships.

REFERENCES

(1) Castner, E. W.; Margulis, C. J.; Maroncelli, M.; Wishart, J. F. Ionic Liquids: Structure and Photochemical Reactions. *Annu. Rev. Phys. Chem.* **2011**, *62*, 85.
(2) Davis, J. H. University Of South Alabama. *Functionalized Ionic Liquids, and Methods of Use Thereof.* EP2258706 A3, 2007.
(3) Pez, G. P.; Carlin, R. T. Air Products And Chemicals, Inc.. *Method for Gas Separation.* U.S. Patent US4761164 A, 1986.
(4) Plechkova, N. V.; Seddon, K. R. Applications of Ionic Liquids in the Chemical Industry. *Chem. Soc. Rev.* **2008**, *37*, 123.
(5) Torralba-Calleja, E.; Skinner, J.; Gutierrez-Tauste, D. CO_2 Capture in Ionic Liquids: A Review of Solubilities and Experimental Methods. *J. Chem.* **2013**, *2013*, 16.
(6) Condemarin, R.; Scovazzo, P. Gas Permeabilities, Solubilities, Diffusivities, and Diffusivity Correlations for Ammonium-Based Room Temperature Ionic Liquids with Comparison to Imidazolium and Phosphonium RTIL Data. *Chem. Eng. J.* **2009**, *147*, 51.
(7) Moya, C.; Palomar, J.; Gonzalez-Miquel, M.; Bedia, J.; Rodriguez, F. Diffusion Coefficients of CO_2 in Ionic Liquids Estimated by Gravimetry. *Ind. Eng. Chem. Res.* **2014**, *53*, 13782.
(8) Camper, D.; Becker, C.; Koval, C.; Noble, R. Diffusion and Solubility Measurements in Room Temperature Ionic Liquids. *Ind. Eng. Chem. Res.* **2006**, *45*, 445.
(9) Kortenbruck, K.; Pohrer, B.; Schluecker, E.; Friedel, F.; Ivanovic-Burmazovic, I. Determination of the Diffusion Coefficient of CO_2 in the Ionic Liquid Emim NTf$_2$ Using Online FTIR Measurements. *J. Chem. Thermodyn.* **2012**, *47*, 76.
(10) Kenkre, V. M.; Tokmakoff, A.; Fayer, M. D. Theory of Vibrational Relaxation of Polyatomic Molecules in Liquids. *J. Chem. Phys.* **1994**, *101*, 10618.
(11) Lin, Y. S.; Ramesh, S. G.; Shorb, J. M.; Sibert, E. L.; Skinner, J. L. Vibrational Energy Relaxation of the Bend Fundamental of Dilute Water in Liquid Chloroform and D-Chloroform. *J. Phys. Chem. B* **2008**, *112*, 390.
(12) Imoto, S.; Xantheas, S. S.; Saito, S. Ultrafast Dynamics of Liquid Water: Energy Relaxation and Transfer Processes of the OH Stretch and the HOH Bend. *J. Phys. Chem. B* **2015**, *119*, 11068.
(13) Rey, R.; Hynes, J. T. Tracking Energy Transfer from Excited to Accepting Modes: Application to Water Bend Vibrational Relaxation. *Phys. Chem. Chem. Phys.* **2012**, *14*, 6332.
(14) Rey, R.; Ingrosso, F.; Elsaesser, T.; Hynes, J. T. Pathways for H_2O Bend Vibrational Relaxation in Liquid Water. *J. Phys. Chem. A* **2009**, *113*, 8949.
(15) Seki, T.; Grunwaldt, J.-D.; Baiker, A. In Situ Attenuated Total Reflection Infrared Spectroscopy of Imidazolium-Based Room-

DOI: 10.1021/acs.jpcb.5b11454
J. Phys. Chem. B 2016, 120, 549−556

Temperature Ionic Liquids under "Supercritical" CO_2. *J. Phys. Chem. B* **2009**, *113*, 114.
(16) Venyaminov, S. Y.; Prendergast, F. G. Water (H_2O and D_2O) Molar Absorptivity in the 1000−4000 cm^{-1} Range and Quantitative Infrared Spectroscopy of Aqueous Solutions. *Anal. Biochem.* **1997**, *248*, 234.
(17) Fenn, E. E.; Wong, D. B.; Fayer, M. D. Water Dynamics in Small Reverse Micelles in Two Solvents: Two-Dimensional Infrared Vibrational Echoes with Two-Dimensional Background Subtraction. *J. Chem. Phys.* **2011**, *134*, 054512.
(18) Karthick Kumar, S. K.; Tamimi, A.; Fayer, M. D. Comparisons of 2D IR Measured Spectral Diffusion in Rotating Frames Using Pulse Shaping and in the Stationary Frame Using the Standard Method. *J. Chem. Phys.* **2012**, *137*, 184201.
(19) Nishida, J.; Tamimi, A.; Fei, H.; Pullen, S.; Ott, S.; Cohen, S. M.; Fayer, M. D. Structural Dynamics inside a Functionalized Metal−Organic Framework Probed by Ultrafast 2D IR Spectroscopy. *Proc. Natl. Acad. Sci. U. S. A.* **2014**, *111*, 18442.
(20) Garrett-Roe, S.; Hamm, P. Purely Absorptive Three-Dimensional Infrared Spectroscopy. *J. Chem. Phys.* **2009**, *130*, 164510.
(21) Wong, D. B.; Giammanco, C. H.; Fenn, E. E.; Fayer, M. D. Dynamics of Isolated Water Molecules in a Sea of Ions in a Room Temperature Ionic Liquid. *J. Phys. Chem. B* **2012**, *117*, 623.
(22) Kramer, P. L.; Giammanco, C. H.; Fayer, M. D. Dynamics of Water, Methanol, and Ethanol in a Room Temperature Ionic Liquid. *J. Chem. Phys.* **2015**, *142*, 212408.
(23) Brinzer, T.; Berquist, E. J.; Ren, Z.; Dutta, S.; Johnson, C. A.; Krisher, C. S.; Lambrecht, D. S.; Garrett-Roe, S. Ultrafast Vibrational Spectroscopy (2D-IR) of CO_2 in Ionic Liquids: Carbon Capture from Carbon Dioxide's Point of View. *J. Chem. Phys.* **2015**, *142*, 212425.
(24) Schmidt, J. R.; Corcelli, S. A.; Skinner, J. L. Pronounced Non-Condon Effects in the Ultrafast Infrared Spectroscopy of Water. *J. Chem. Phys.* **2005**, *123*, 044513.
(25) Yuan, R.; Yan, C.; Tamimi, A.; Fayer, M. D. Molecular Anion Hydrogen Bonding Dynamics in Aqueous Solution. *J. Phys. Chem. B* **2015**, *119*, 13407.
(26) Park, S.; Kwak, K.; Fayer, M. D. Ultrafast 2D-IR Vibrational Echo Spectroscopy: A Probe of Molecular Dynamics. *Laser Phys. Lett.* **2007**, *4*, 704.
(27) Fayer, M. D.; Zheng, J. R.; Kwak, K. Ultrafast Chemical Exchange 2-D Infrared Spectroscopy of Complexes in Solution. *Abstr. Pap. Am. Chem. Soc.* **2006**, *231*.
(28) Gallagher Faeder, S. M.; Jonas, D. M. Two-Dimensional Electronic Correlation and Relaxation Spectra: Theory and Model Calculations. *J. Phys. Chem. A* **1999**, *103*, 10489.
(29) Asbury, J. B.; Steinel, T.; Stromberg, C.; Gaffney, K. J.; Piletic, I. R.; Goun, A.; Fayer, M. D. Ultrafast Heterodyne Detected Infrared Multidimensional Vibrational Stimulated Echo Studies of Hydrogen Bond Dynamics. *Chem. Phys. Lett.* **2003**, *374*, 362.
(30) Falk, M.; Miller, A. G. Infrared Spectrum of Carbon Dioxide in Aqueous Solution. *Vib. Spectrosc.* **1992**, *4*, 105.

DOI: 10.1021/acs.jpcb.5b11454
J. Phys. Chem. B 2016, 120, 549−556